LAWRENCE
LIVERMORE
NATIONAL
LABORATORY

LLNL-CONF-863380

# Design and Characterization of the Time-Resolved Spectrometer (OpSpecTR) for the NIF Iron Opacity Campaign

Y. P. Opachich, B. Golick, J. G. Buscho, A. Carpenter, B. T. Funsten, A. M. Garafalo, J. Heinmiller, E. C. Dutra, R. Knight, D. Max, D. C. Mayes, S. B. Morioka, K. J. Moy, P. R. Nyholm, A. E. Peterson, R. B. Petre, R. S. Posadas, A. M. Sharp, W. Stolte, V. Tran, S. D. Trent, M. S. Wallace, D. E. Winget, T. S. Perry, T. J. Urbatsch, R. F. Heeter

April 22, 2024

High Temperature Plasma Diagnostics
Asheville, NC, United States
April 21, 2024 through April 25, 2024

## Disclaimer

# Design and Characterization of the Time-Resolved Opacity Spectrometer (OpSpecTR) for the NIF Iron Opacity Campaign

Y. P. Opachich,[1] B. Golick,[1] J. G. Buscho,[1] A. C. Carpenter,[1] B. T. Funsten,[1] A. M. Garafalo,[1] J. Heinmiller,[3] E. C. Dutra,[3] R. Knight,[3] D. Max,[3] D. C. Mayes,[5] S. B. Morioka,[1] K. J. Moy,[4] P. R. Nyholm,[1] A. E. Peterson,[3] R. B. Petre,[1] R. S. Posadas,[1] A. M. Sharp,[1] V. Tran,[3] S. D. Trent,[3] M. S. Wallace,[3] D. E. Winget,[5] T. S. Perry,[2] T. J. Urbatsch,[2] and R. F. Heeter[1]

[1]*Lawrence Livermore National Laboratory, Livermore, CA 94550, USA*
[2]*Los Alamos National Laboratory, NM 87545, USA*
[3]*Nevada National Security Sites, Livermore, California 94550, USA*
[4]*Nevada National Security Sites, Santa Barbara, California 93117, USA*
[5]*University of Texas at Austin, TX 78712, USA*

(Presented XXXXX; received XXXXX; accepted XXXXX; published online XXXXX)

A new time-resolved opacity spectrometer (OpSpecTR) is currently under development for the National Ignition Facility (NIF) opacity campaign. The spectrometer utilizes Icarus version 2 (IV2) hybridized complementary metal-oxide semiconductor (hCMOS) sensors to collect gated data at the time of the opacity transmission signal, unlocking the ability to collect higher-temperature measurements on NIF. Experimental conditions to achieve higher temperatures are feasible; however, backgrounds will dominate the data collected by the current time-integrating opacity spectrometer (OpSpec). The shortest available OpSpecTR integration time of approximately 2 ns is predicted to reduce self-emission and other late-time backgrounds by up to 80%. Initially, three Icarus sensors will be used to collect data in the self-emission, backlighter, and absorption regions of the transmission spectrum, with plans to upgrade to five Daedalus sensors in future implementations with integration times of approximately 1.3 ns. We present the details of the diagnostic design along with recent characterization results of the IV2 sensors.

## I. OVERVIEW

Experimentally obtained x-ray opacities of elements like oxygen and iron are crucial for radiation-hydrodynamic codes that are widely used to understand various astrophysical phenomena in the solar interior and stellar evolution.[1-3] Achieving laboratory conditions akin to those in astrophysical environments, such as the typical temperatures ranging between 120-210 eV in the outer solar convection zone, presents significant challenges. Nonetheless, recent efforts have demonstrated the feasibility of acquiring experimental data at such elevated temperatures. Opacity measurements of these elements have been carried out at the NIF[4] in Lawrence Livermore National Lab and the Z-facility in Sandia National Laboratories[5-10]. These studies have revealed a notable inconsistency between measured and predicted opacities in iron, as described in Bailey et al.,[5] particularly accentuated at temperatures above 164 eV.

The NIF opacity campaign has developed a platform and has been routinely collecting iron and oxygen data at lower temperatures, with plans underway for opacity measurements at higher temperatures and densities in the near future. Unfortunately, accessing higher temperatures in our experiment requires an increase in the laser energy deposited into the hohlraum. Several experiments have been performed to evaluate the data quality at higher temperatures. These measured background levels that dominated the backlighter signal, necessitating the implementation of new gated diagnostic to enhance signal-to-noise ratios.

In this manuscript, we elaborate on the design, initial characterization and future implementation of a new time-resolved opacity spectrometer. This instrument is poised to facilitate the extension of opacity measurements to temperatures well above 164 eV.

## II. EXPERIMENTAL SETUP

The NIF opacity experimental platform comprises a laser-driven target[11-13] consisting of a vacuum-filled CH capsule backlighter, a conical collimator and a laser driven "Apollo"[8] hohlraum used to heat samples. The opacity target is shown in Figure 1. Three shields are strategically positioned on the hohlraum and near the backlighter to minimize diagnostic exposure to laser light and plasma emission from the laser entrance holes and backlighter. During the experiment, up to 96 NIF laser beams implode the capsule, producing a ~300 ps full width at half max (FWHM) burst of broad band x-ray radiation. The backlighter x-ray emission passes through the collimator, the laser-driven hohlraum containing the heated sample, and

[a)]Author to whom correspondence should be addressed: opachich1@llnl.gov

finally onto the time-integrating opacity spectrometer (OpSpec)[14-17].

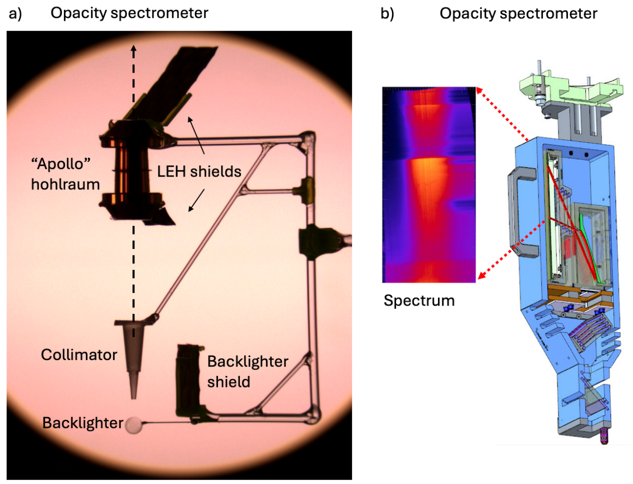


FIG.1. a) Opacity Target. The target comprises a vacuum filled (2 mm diameter CH shell) backlighter, a conical collimator, a hohlraum and three shields to obscure plasma emission from the laser entrance holes and backlighter. b) OpSpec is shown along with a collected oxygen spectrum.

The time integrating OpSpec utilizes two elliptically bent crystals designed to collect duplicate spectra, with data typically recorded on image plates (IP) or film. Figure 2 displays an example oxygen spectrum collected in the 1000-2000 eV range. The sample is positioned off-axis in the hohlraum, generating three spectral regions: an absorption region, an $I_0$ region provided by the recorded backlighter signal, and a self-emission region. While opacity determination conventionally involves taking a line-out through the absorption region and normalizing it by the backlighter ($I_0$)[8,18], the time-integrated spectrum also captures background emission. Various sources contribute to this background, primarily the laser entrance hole (LEH) window, the tamper, the sample self-emission and hohlraum blowoff. Higher hohlraum temperature exacerbate the background, until it overwhelms the recorded transmission and backlighter spectra. Unfortunately, this compromises data integrity and complicates analysis.

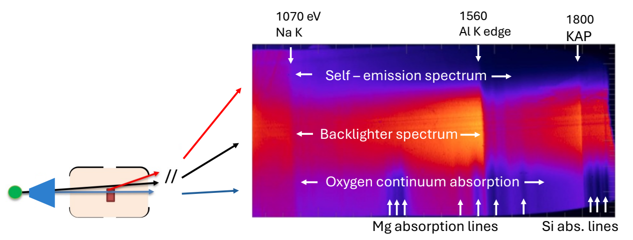


FIG 2. From left to right, a close-up of the backlighter and collimator is shown, followed by a schematic of the hohlraum and recorded transmission spectrum. The spectrum is divided into the self-emission region, backlighter region, and the absorption region seen at the bottom of the spectrum. Recorded Mg and Si absorption lines are marked at the bottom, the Na K and Al K edge, and KAP absorption are shown for reference.

With recent development of fast gated hCMOS sensors by Sandia National Laboratories[19], it has become possible to gate out a significant portion (up to 80%) of the background contributions. Figure 3 illustrates an example of measured hohlraum emission time history. On average the emission lasts ~15 ns, contributing to total background. The emission can be separated in early and late time, occurring before and after the backlighter signal. The LEH window emission was simulated by E. Dodd et al.[12] It was found that CH emission is only significant early in time, prior to the picket on the laser pulse blowing apart the LEH window. The low-density CH plasma formed from the LEH window does not emit significantly in the 1.0-2.0 keV X-ray band after ~2 ns. In addition, hohlraum-only shots performed to measure the emission background show modest late-time hohlraum blowoff contributions at current drive levels (130-160 eV sample temperatures). However, shots with higher drive levels have shown progressively increasing backgrounds, and increased nonuniformity across the spectrometer, consistent with substantially increased hohlraum blowoff background contributions moving in from large radius into the spectrometer field of view.

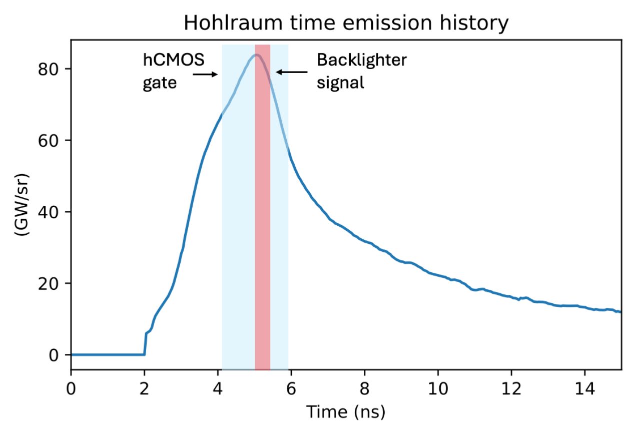


FIG 3: Opacity hohlraum time emission history. The overall hohlraum emission is shown in blue. The 2 ns hCMOS gate window and ~300 ps backlighter signal are shown in light blue and red respectively.

The backlighter is timed to emit when the sample temperature is constant providing transmission spectra covering a few hundred picoseconds. By setting the IV2 sensor gate to the shortest available integration time (2.5 ns), much of the background can be rejected. We anticipate up to 80% reduction in background generated by the LEH window and hohlraum blowoff, as discussed previously, this contribution occurs early (before 2 ns) and late (after 6 ns) in the laser drive respectively. Meanwhile, the tamper and sample self-emission contributions are expected to decrease by 50%. This estimate is based on measurements that have shown that the foil temperature is almost the same as the hohlraum temperature[20], so the sample self-emission flux should have a similar time-history (but at different amplitude) as the DANTE-2 flux shown in Figure 3. The opacity coefficient of absorption (κ) tends to increase as temperature decreases, overweight the sample emission early and late in time. Based on this, Figure 3 provides a conservative estimate of the relative sample emission at times outside the 2ns gate. Based on the emission shown in the figure, a 2 - 3 ns gate is narrow enough to clip out at least 50% of the sample emission background.

## III. DESIGN AND REQUIREMENTS

The time resolved opacity spectrometer extends the original OpSpec design by converting one of the x-ray channels to record time resolved spectra (see Figure 4). The first optical path remains dedicated to capturing a spectrum on film or image plate, much like in the original diagnostic. The newly upgraded channel includes a grazing incidence x-ray mirror and a new elliptical crystal that disperses photons onto three hCMOS sensors to capture a gated spectrum. The grazing incidence mirror, fabricated by InSync, Inc.,[21] utilizes a 15 mm thick, Au coated Si substrate with better than 3 Å surface roughness. The design of the elliptical crystal is described elsewhere; for further details, refer to publications by M. Wallace RSI[17]. By adjusting the angle of the mirror, crystal geometry, and material, we can tailor the spectral coverage from 0.5 to 6 keV. Our initial design will utilize a standard KAP crystal, providing coverage from 1 to 2 keV. The fast-gating Icarus v2 (IV2)[22,23] Daedalus v2 (DV2)[24] sensors are designed and fabricated at Sandia National Laboratories. Initially, we will utilize IV2 sensors due to availability and easier integration into the facility, owing to their prior diagnostic use, with plans to upgrade to DV2 sensors in future iterations. Both IV2 and DV2 sensors feature a resolution of 0.5 MP, with 25 x 25 μm pixel size and 8 μm diode thickness. The pixelated sensor consists of imaging diodes[25] bonded to a Readout Integrated Circuit (ROIC) substrate facilitating the capture, storage and read out of output from individual photodiode. Icarus sensors offer four imaging frames, with the fastest option of ~2 ns integration time and ~2 ns frame separation. Meanwhile, Daedalus sensors feature a 1.5 ns integration time and 1-2 ns interframe separation.

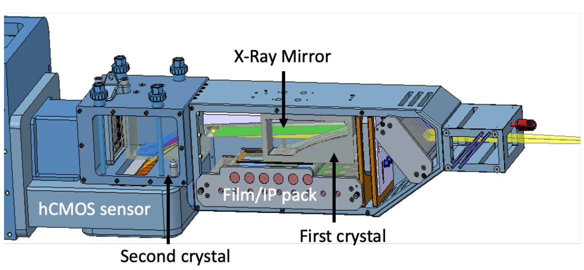


FIG 4: OpSpecTR model illustrating two x-ray channels. The upgraded OpSpecTR incorporates a grazing incidence x-ray mirror, an elliptical crystal and three hCMOS sensors.

Three co-timed hCMOS sensors will cover the three spectral regions, as depicted in Figure 5. Both IV2 and DV2 sensors meet OpSpecTR requirements, detailed in Table 1. In addition to background reduction, the use of hCMOS sensors is expected to enhance spectral resolution by up to a factor of two over image plate media, as image plates typically have spatial resolution of 50 μm.[26] In addition, the sensor provides better spectral coverage, with improvement in quantum efficiency at lower energies in comparison with image plates.[27]

Camera boards are designed and built at LLNL[28]. The boards offer partial vacuum compatibility for integration within a Diagnostic Insertion Manipulator (DIM) and are radiation hardened to ensure compatibility with higher-yield experiments. On-board temperature and pressure monitoring capabilities are available. DV2 sensors will include a built-in temperature monitor, which is essential for operating in vacuum environments.

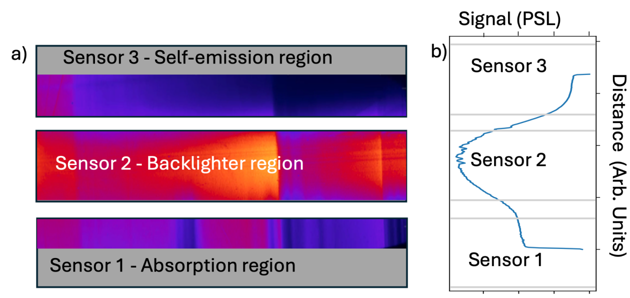


FIG 5: a) Proposed sensor layout, depicting three hCMOS sensors capturing three regions of the opacity spectrum. b) Lineout of the opacity signal with sensor overlay.

OpSpecTR also incorporates a 445 nm laser-diode fiducial attached to 105 nm multi-mode fiber-optic assembly, producing an output of ~900 pJ with a pulse-width of ~125 ps. The laser-diode output is routed to a 1x6 fiber optic splitter and then directed to the sensors using a fiber graded-index (grin) lens assembly, which transmits light orthogonal to the fiber. This fiber system will allow users to verify sensor operation, timing, and testing while installed in a DIM. Additionally, a photodiode (AXUVHS) is placed at the rear wall of the detector cavity to monitor overall photon flux.

TABLE 1. Specifications of hCMOS sensors critical for OpSpecTR.

| Type | Specification |
|---|---|
| Image Dimension | 0.5 megapixels |
| Gating timing | 1.2 ns (DV2) – 2.5 ns (IV2) |
| Sensitivity | x-ray from 300 eV to 20 keV |
| Spatial Resolution | 25 x 25 μm |
| Full Well | 500 thousand to 1.5 million e- |
| Dynamic range | 1000:1 (IV2) and 3300:1 (DV2) |

## IV. SENSOR CHARACTERIZATION

The performance of Icarus sensors can vary between fabrication batches. To ensure reliability, each sensor undergoes rigorous testing before integration into a diagnostic system. Initial testing typically includes standard acceptability assessmenets[24,29], followed by diagnostic specific evaluations. The OpSpecTR diagnostic has several key performance requirements, including quantum efficiency (QE) in the 300 eV to ~5 keV range, spatial resolution, dynamic range/linearity, and gate integration time. In addition, the characterization and mitigation of background oscillations are essential.[30]

Quantum efficiency characterization was performed at the Stanford Synchrotron Radiation Light source (SSRL) soft x-ray (SXR) beam line 16-2, by the Nevada National Security Sites. A 40 x 20 pixel beam spot was incident onto the sensor, that was set to a manual integration time of 100 µs to provide enough photons/pixel for adequate Poisson statistics. The resulting measured QE along with a calculated energy absorbed curve is shown in Figure 6. The QE extends down to approximately 300 eV, representing a significant improvement over image plate sensitivity[27]. This improvement will be significant for future Fe and O opacity measurements.

The gate width of IV2 sensors was measured at LLNL.[29,31] On average IV2 sensors exhibit a 2.4 ns gate width and a 3 ns gate to gate separation on the 2_2 timing mode. In this mode the gate integration time is nominally 2 ns with a 2 ns inter-frame separation. We expect that utilizing a 2.4 ns gate will effectively remove a large portion of early and late time background sources. In the future, DV2 sensors, with gate widths as short as 1.4 ns, will be used to further reduce background.

Previous characterizations of IV2 sensor performance, as demonstrated by Looker et al,[23] have shown no discernable blurring of images. However, diode signal non-uniformity is sizable, with ~20% variation in counts for an average count of around 1000. To mitigate this issue, we plan to average over ~ 4 pixels in our data analysis, effectively setting our detector spatial resolution to ~50 µm. Variation in sensitivity will be further investigated in the soft x-ray range.

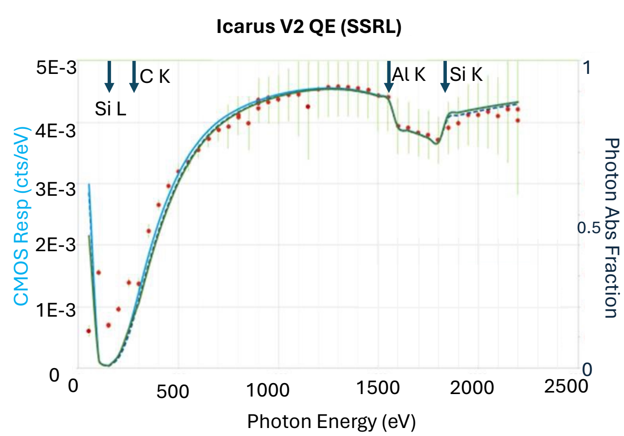


FIG. 6: QE of IV2 sensor. The collected IV2 QE is shown in orange points, calculated absorbed photon fraction is shown for several layer thicknesses in solid lines. TheSi L, C K, Al K and Si K edges are shown for reference.

Background oscillations were characterized using a 532 nm, 3 ns laser pulse. The study focused on testing various masking patterns for background oscillation mitigation.[30] The results revealed that the contribution of background oscillations can be reduced to below 1% of peak signal counts through the use of masking patterns that block 60% or more of total incident photons, this work is in agreement with previous studies[30]. An example mask is shown in Figure 7, alongside background oscillation levels, the original signal counts and the subtracted region counts.

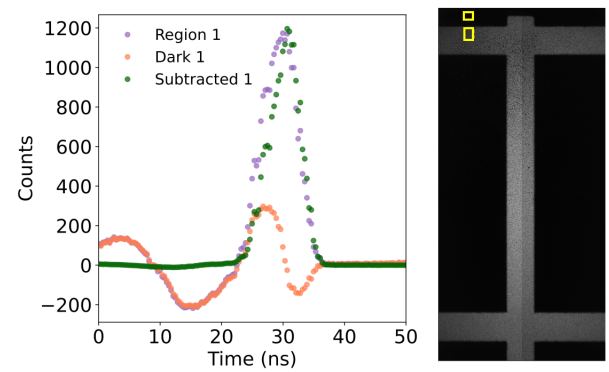


FIG 7: Example of a test mask used to reduce background oscillations, along with an analysis resulting from signal and background regions shown in the top-left portion of the image.

## IV. FUTURE WORK

The fabrication of parts for OpSpecTR are nearing completion, and we are beginning to build the diagnostic. Diagnostic assembly and offline calibration are expected to be finished by mid-2024. Initial diagnostic timing shots on NIF are scheduled for late 2024, with the first opacity data to be obtained in 2025.

## V. CONCLUSIONS

A new time-resolved spectrometer (OpSpecTR) is being developed for the NIF opacity campaign. The spectrometer employs Icarus version 2 hCMOS sensors to collect gated data at the time of the opacity transmission signal. The use of fast gated sensors reduces hohlraum and sample emission backgrounds, enabling the collection of transmission spectra at higher temperatures on NIF. Sensor performance has been characterized, and efforts are now shifting to building, characterizing and commissioning the OpSpecTR diagnostic for its initial use on NIF.

## V. ACKNOWLEDGMENTS

This work was performed under the auspices of the U. S. Department of Energy by Lawrence Livermore National Laboratory under contract DE-AC52-07NA27344, by Los Alamos National Laboratory under contract 89233218CNA000001. LLNL-CONF-863380 and by the Nevada National Security Sites, Mission Support and Test

Services under contract DE-NA0003624. LLNL-CONF-863380.

The data that support the findings of this study are available from the corresponding author upon reasonable request.

## VI. REFERENCES


[1] Winget, D. E. *et al.* An Independent Method for Determining the Age of the Universe. *The Astrophysical Journal* **315**, L77 (1987). https://doi.org/10.1086/184864

[2] Basu, S. & Antia, H. M. Helioseismology and solar abundances. *Physics Reports* **457**, 217-283 (2008). https://doi.org/https://doi.org/10.1016/j.physrep.2007.12.002

[3] Blancard, C., Cossé, P. & Faussurier, G. Solar mixture opacity calculations using detailed configuration and level accounting treatments. *The Astrophysical Journal* **745**, 10 (2011). https://doi.org/10.1088/0004-637x/745/1/10

[4] Miller, G. H., Moses, E. I. & Wuest, C. R. The National Ignition Facility: enabling fusion ignition for the 21st century. *Nuclear Fusion* **44**, S228 (2004).

[5] Bailey, J. E. *et al.* A higher-than-predicted measurement of iron opacity at solar interior temperatures. *Nature* **517**, 56-59 (2015). https://doi.org/10.1038/nature14048

[6] Bailey, J. E. *et al.* Iron-Plasma Transmission Measurements at Temperatures Above 150 eV. *Physical Review Letters* **99**, 265002 (2007).

[7] Bailey, J. E. *et al.* Experimental investigation of opacity models for stellar interior, inertial fusion, and high energy density plasmasa). *Physics of Plasmas* **16**, 058101 (2009). https://doi.org/doi:http://dx.doi.org/10.1063/1.3089604

[8] Heeter, R. F. *et al.* Conceptual design of initial opacity experiments on the national ignition facility. *Journal of Plasma Physics* **83**, 595830103 (2017). https://doi.org/10.1017/S0022377816001173

[9] Perry, T. S. *et al.* Progress toward NIF opacity measurements. *High Energy Density Physics* **35**, 100728 (2020). https://doi.org/https://doi.org/10.1016/j.hedp.2019.100728

[10] Perry, T. S. *et al.* Replicating the Z iron opacity experiments on the NIF. *High Energy Density Physics* **23**, 223-227 (2017). https://doi.org/https://doi.org/10.1016/j.hedp.2017.05.006

[11] Cardenas, T. *et al.* Design and Fabrication of Opacity Targets for the National Ignition Facility. *Fusion Science and Technology* **73**, 458-466 (2018). https://doi.org/10.1080/15361055.2017.1389559

[12] Dodd, E. S. *et al.* Hohlraum modeling for opacity experiments on the National Ignition Facility. *Physics of Plasmas* **25**, 063301 (2018). https://doi.org/10.1063/1.5026285

[13] Opachich, Y. P. *et al.* Capsule implosions for continuum x-ray backlighting of opacity samples at the National Ignition Facility. *Physics of Plasmas* **24**, 063301 (2017). https://doi.org/10.1063/1.4985076

[14] King, J. A. *et al.* Implementation of a 1-2 keV point-projection x-ray spectrometer on the National Ignition Facility. *Review of Scientific Instruments* **89**, 10F101 (2018). https://doi.org/10.1063/1.5038092

[15] Ross, P. W. *et al.* Design of the opacity spectrometer for opacity measurements at the National Ignition Facility. *Review of Scientific Instruments* **87**, 11D623 (2016). https://doi.org/10.1063/1.4962819

[16] Wallace, M. S. *et al.* Upgrades and redesign of the National Ignition Facility's soft x-ray opacity spectrometer (OpSpec). *Review of Scientific Instruments* **92** (2021). https://doi.org/10.1063/5.0043517

[17] Wallace, M. S. *et al.* Sub-keV design for the National Ignition Facility's soft x-ray Opacity Spectrometer (OpSpec) and expansion plans for time-resolved measurements. *Review of Scientific Instruments* **93** (2022). https://doi.org/10.1063/5.0101704

[18] Perry, T. S. *et al.* Quantitative measurement of mid-z opacities. *Journal of Quantitative Spectroscopy and Radiative Transfer* **54**, 317-324 (1995). https://doi.org/http://dx.doi.org/10.1016/0022-4073(95)00066-T

[19] Claus, L. *et al. An overview of the Ultrafast X-ray Imager (UXI) program at Sandia Labs*. Vol. 9591 OPO (SPIE, 2015).

[20] Opachich, Y. P. *et al.* DANTE as a primary temperature diagnostic for the NIF iron opacity campaign. *Rev. Sci. Instrum.* **92** (2021).

[21] InSync, Inc. *http://www.insyncoptics.com*.

[22] Dayton, M. *et al. The electron detection performance of the "Icarus" hCMOS imaging sensor*. Vol. 11838 OPO (SPIE, 2021).

[23] Looker, Q., Colombo, A. P., Kimmel, M. & Porter, J. L. X-ray characterization of the Icarus ultrafast x-ray imager. *Review of Scientific Instruments* **91** (2020). https://doi.org/10.1063/5.0004711

[24] Garafalo, A. *et al. Characterization suite of a 1ns, multi-frame hybridized CMOS imager for the ultra-fast x-ray imager program*. Vol. 12696 OPO (SPIE, 2023).

[25] Looker, Q. *et al.* Superlattice-enhanced silicon soft X-ray and charged particle detectors with nanosecond time response. *Nuclear Instruments and Methods in Physics Research Section A: Accelerators, Spectrometers, Detectors and Associated Equipment* **916**, 148-153 (2019). https://doi.org/https://doi.org/10.1016/j.nima.2018.11.052

[26] Maddox, B. R. *et al.* High-energy x-ray backlighter spectrum measurements using calibrated image plates. *Review of Scientific Instruments* **82**, - (2011). https://doi.org/doi:http://dx.doi.org/10.1063/1.3531979

[27] Haugh, M. J., Lee, J., Romano, E. & Schneider, M. in *Target Diagnostics Pysics and Engineering for Inertial Confinement Fusion II* Vol. 8850 885007-885007-885011 (Proc. SPIE, 2013).

[28] Macaraeg, C., Dayton, M., Funsten, B. & Carpenter, A. *Design of radiation tolerant FPGAs for the LLNL nanosecond gated CMOS camera program*. Vol. 10763 OPO (SPIE, 2018).

[29] Hurd, E. *et al. Performance characterization of a four-frame nanosecond gated hybrid CMOS image sensor*. Vol. 10763 OPO (SPIE, 2018).

[30] Hassard, B. R. *et al.* Analysis and mitigation of an oscillating background on hybrid complementary metal-oxide semiconductor (hCMOS) imaging sensors at the National Ignition Facility. *Review of Scientific Instruments* **94** (2023). https://doi.org/10.1063/5.0165487

[31] Dayton, M. *et al. A characterization technique for nanosecond gated CMOS x-ray cameras*. Vol. 9966 OPO (SPIE, 2016).